Contents lists available at ScienceDirect

Biomedicine & Pharmacotherapy

journal homepage: www.elsevier.com/locate/biopha

Beneficial effect of TLR4 blockade by a specific aptamer antagonist after acute myocardial infarction

Marta Paz-García [a], Adrián Povo-Retana [a], Rafael I. Jaén [a], Patricia Prieto [b], Diego A. Peraza [a], Carlos Zaragoza [c,d], Macarena Hernandez-Jimenez [e], David Pineiro [e], Javier Regadera [f], María L. García-Bermejo [g], E. Macarena Rodríguez-Serrano [g], Sergio Sánchez-García [a], María A. Moro [h], Ignacio Lizasoaín [i], Carmen Delgado [a,d], Carmen Valenzuela [a,d], Lisardo Boscá [a,d,j,*]

[a] Instituto de Investigaciones Biomédicas Alberto Sols, CSIC-UAM, Arturo Duperier 4, 28029 Madrid, Spain
[b] Pharmacology, Pharmacognosy and Botany Department, Faculty of Pharmacy, Complutense University of Madrid, 28040 Madrid, Spain
[c] Departamento de Cardiología, Unidad de Investigación Mixta Universidad Francisco de Vitoria, 28223 Madrid, Spain
[d] Centro de Investigación Biomédica en Red de Enfermedades Cardiovasculares (CIBERCV), Av. Monforte de Lemos 3-5, P-11, 28029 Madrid, Spain
[e] AptaTargets SL, Av del Cardenal Herrera Oria, 298, 28035 Madrid, Spain
[f] Department of Anatomy, Faculty of Medicine, Autonomous University of Madrid, 28029 Madrid, Spain
[g] Instituto Ramón y Cajal de Investigación Sanitaria (IRYCIS), RICORS2040, Ctra de Colmenar Viejo, 28034 Madrid, Spain
[h] Centro Nacional de Investigaciones Cardiovasculares, Melchor Fernández Almagro, 28029 Madrid, Spain
[i] Departamento de Farmacología y Toxicología, Facultad de Medicina Universidad Complutense Madrid, Instituto de Investigación Hospital 12 de Octubre, Madrid, Spain
[j] Unidad de Biomedicina (Unidad Asociada al CSIC) de la Universidad de Las Palmas de Gran Canaria, Las Palmas, Spain

ARTICLE INFO

ABSTRACT

Experimental evidence indicates that the control of the inflammatory response after myocardial infarction is a key strategy to reduce cardiac injury. Cellular damage after blood flow restoration in the heart promotes sterile inflammation through the release of molecules that activate pattern recognition receptors, among which TLR4 is the most prominent. Transient regulation of TLR4 activity has been considered one of the potential therapeutic interventions with greater projection towards the clinic. In this regard, the characterization of an aptamer (4FT) that acts as a selective antagonist for human TLR4 has been investigated in isolated macrophages from different species and in a rat model of cardiac ischemia/reperfusion (I/R). The binding kinetics and biological responses of murine and human macrophages treated with 4FT show great affinity and significant inhibition of TLR4 signaling including the NF-κB pathway and the LPS-dependent increase in the plasma membrane currents (Kv currents). In the rat model of I/R, administration of 4FT following reoxygenation shows amelioration of cardiac injury function and markers, a process that is significantly enhanced when the second dose of 4FT is administered 24 h after reperfusion of the heart. Parameters such as cardiac injury biomarkers, infiltration of circulating in-flammatory cells, and the expression of genes associated with the inflammatory onset are significantly reduced. In addition, the expression of anti-inflammatory genes, such as IL-10, and pro-resolution molecules, such as resolvin D1 are enhanced after 4FT administration. These results indicate that targeting TLR4 with 4FT offers new therapeutic opportunities to prevent cardiac dysfunction after infarction.

1. Introduction

The myocardial tissue is composed of cardiomyocytes (25–35% of cells and around 70–80% of the tissue volume), cardiac fibroblasts, endothelial cells, smooth muscle cells, and immune cells, which are present as homeostatic resident cells. Both myocytes and non-myocytic cells actively respond to pathogenic situations coordinating the immune response [1].

After an acute myocardial infarction (MI), neutrophils, monocytes/macrophages, and endothelial cells sense these injury-released

molecules, which promote the increased expression of inflammatory mediators [2], activating the endothelial permeability and immune cell infiltration into the myocardium [3,4]. During cardiac ischemia/reperfusion (I/R), an enhanced infiltration of inflammatory leukocytes occurs, which contributes to the removal of dead cardiomyocytes. However, the adult mammalian heart has insufficient regenerative capacity; hence, a reparative process is activated to replace these dead cardiomyocytes with scar tissue and promote a rapid pro-inflammatory response [5,6]. Interestingly, it was demonstrated that leukocytes are necessary for a proper resolution of inflammation and fibrotic scar formation [7,8]. Thus, a correct switch between the inflammatory and reparative response is necessary since the depletion of neutrophils or macrophages induces greater damage [6,9].

Regarding inflammation, the Toll-like receptor TLR4 is widely expressed in many cell types and it is well known for its implication in cardiovascular diseases (CVDs) [10,11]. Excessive TLR4 activation disrupts the immune homeostasis in the host as dead cardiomyocytes release pro-inflammatory cytokines that activate and attract more leukocytes. This secretion of inflammatory cytokines and chemokines is a hallmark associated with the development of heart failure [12–15]. In agreement with this, *Tlr4* deficient mice show a lower inflammatory response with a decrease in the NF-κB signaling pathway after myocardial I/R injury [16]. Consequently, these animals show a lower cardiac inflammatory infiltration and infarct size when compared with *wild-type* counterparts [2,17–19]. One possibility to modulate TLR4 activity is using selective aptamer antagonists. Aptamers are short single-stranded oligonucleotides (20–100 nucleotides) of DNA or RNA (ssDNA, ssRNA) that are characterized by having a specific and complex three-dimensional structure (for a review, see [20–22]). These molecules bind to their target by conformational compatibility. To ensure specificity, aptamers are generated *in vitro* by Systematic Evolution of Ligands by Exponential Enrichment (SELEX) technology [23]. The function of aptamers is similar to antibodies because they recognize and bind to a preselected target in a specific way [24–27]. The specificity is based on the three-dimensional structure that the sequence acquires. The specificity and high affinity of aptamers for their targets are comparable to that of antibodies but, due to their size, aptamers can access epitopes or tissues that antibodies cannot [26]. Accordingly, here we have characterized the protective effects against cardiac ischemia/reperfusion injury of an aptamer that blocks specifically TLR4 signaling.

2. Materials and methods

2.1. Materials

Reagents were from Sigma-Aldrich-Merck (Madrid, ES) or Roche (Darmstadt, DE). Murine or human cytokines were purchased from PeproTech (London, UK). Antibodies were from Abcam (Cambridge, UK) or Cell Signaling (Danvers, MA, USA). Reagents for electrophoresis were from Bio-Rad (Madrid, ES). Tissue culture dishes were from Falcon (Lincoln Park, NJ, USA), and serum and culture media were from Invitrogen (Life Technologies/Thermo-Fisher, Madrid, ES). The aptamer (4FT, ApTOLL; a human TLR4 antagonist), provided by AptaTargets S.L. and stored lyophilized. The sequence and characterization have been previously reported [28]. After resuspension in PBS containing 1 mM MgCl$_2$, it was structured by heat-cold incubation (10 min at 90ºC followed by 10 min at 4ºC) before use.

2.2. Cell procedures

Human macrophages (hMφ) were prepared from buffy coats of blood from healthy anonymous donors from the Centro de Transfusión de la Comunidad de Madrid (Madrid, ES). All the participants provided written consent following the ethical guidelines of the 1975 Declaration of Helsinki and the Committee for Human Subjects (28504/000011). Blood from *Macaca mulatta* was provided by AptaTargets S.L. and

monocytes were processed as the human counterparts following previous protocols [29,30]. Monocytes were differentiated into macrophages and maintained in RPMI 1640 medium (Lonza; Basel, CH) supplemented with heat-inactivated 10% FBS (fetal bovine serum; Sigma) and antibiotics (100 unit/ml penicillin, streptomycin; Sigma). Murine peritoneal macrophages were obtained by peritoneal wash, following previous protocols [31]. Macrophages were maintained in RPMI 1640 medium supplemented with 2% FBS and antibiotics. The incubation chamber conditions were 37ºC with 5% CO$_2$.

2.3. Cell lines

The cardiomyocytic cell lines HL-1 (mouse), H9c2 (rat) and AC16 (human) were cultured in Claycomb medium from Sigma (HL-1) or Dulbecco's Modified Eagle's Medium (DMEM; Lonza) supplemented with heat-inactivated 10% FBS and antibiotics (100 unit/ml penicillin and streptomycin), following previous protocols [32,33].

2.4. Animal experimentation

Animals were cared for according to the protocol approved by the Ethical Committee of our institution (following directive 2010/63/EU of the European Parliament and Recommendation 2007/526/EC regarding the care of experimental animals, enforced in Spanish law under Real Decreto 53/2013, and approved by the Institutional Ethics Committee (PROEX 197/18). Animals were housed *ad libitum* in an environment with maintained temperature and relative humidity and a light/dark cycle (12 h light/12 h dark). Rat myocardial infarction (ischemia/reperfusion model I/R) was done in Sprague-Dawley male rats (200–250 g) supplied by Charles River (Sant Cugat del Valles, ES). Rats were divided into four groups: Sham (n = 12); myocardial I/R followed by saline buffer administration 10 min after reperfusion (I/R; n = 37), myocardial I/R followed by administration of 4FT 10 min after reperfusion (I/R+4FT) (n = 36), myocardial I/R followed by administration of 4FT 10 min and 24 h after reperfusion (I/R+2×4FT) (n = 20). To perform I/R, rats were anesthetized by inhalation of sevoflurane (3–4%; O$_2$ 1%). The temperature was maintained with a warm pad. Before the surgical process started, tramadol (Adolonta; 100 mg/kg) was injected subcutaneously as postoperative analgesia. Rats were ventilated by endotracheal intubation using a ventilator (New England Medical Instruments, Model 121/1; 55 breaths per min; 2.5 ml; Chelmsford, MA). Rats were continuously monitored by a pulse oximeter that controls the heart rate and blood oxygen levels. An incision was made parallel to the lower costal margin. The left pectoralis major muscle was cut up and the ribs were exposed. To reach the anterior surface of the heart, a left thoracotomy was performed, and a retractor was used to expand the ribs. The left anterior descending artery (LAD) was occluded with a blue propylene monofilament surgical non-absorbable suture 6/0 and a propylene tube (PE-10). LAD occlusion was confirmed by the dramatic color change (red to pallor) and restricted ventricular motion. After 30 min of ligation, the tube and suture were removed initiating the reperfusion for 24 h, 72 h or 7 days. The chest was closed with silk non-absorbable suture 4/0. 4FT was administered by tail vein injection of 25 nmol/kg body weight; controls received vehicle (PBS and 1 mM MgCl$_2$). Rats were monitored until spontaneous recovery. The sham-operate group underwent the same surgical procedure without LAD ligation. After 24 h post-surgery tramadol was injected subcutaneously in all groups (Fig. 4A).

2.5. Transthoracic echocardiographic evaluation

M-mode echocardiography was employed to assess cardiac function before and after surgery. Rats were anesthetized by inhalation of sevoflurane (3–4%; O$_2$ 1%). After chest shaving, warm ultrasound transmission gel was applied and cardiac function was analyzed with a high-frequency micro-ultrasound system (Vivid Q, GE Healthcare, IL, USA).
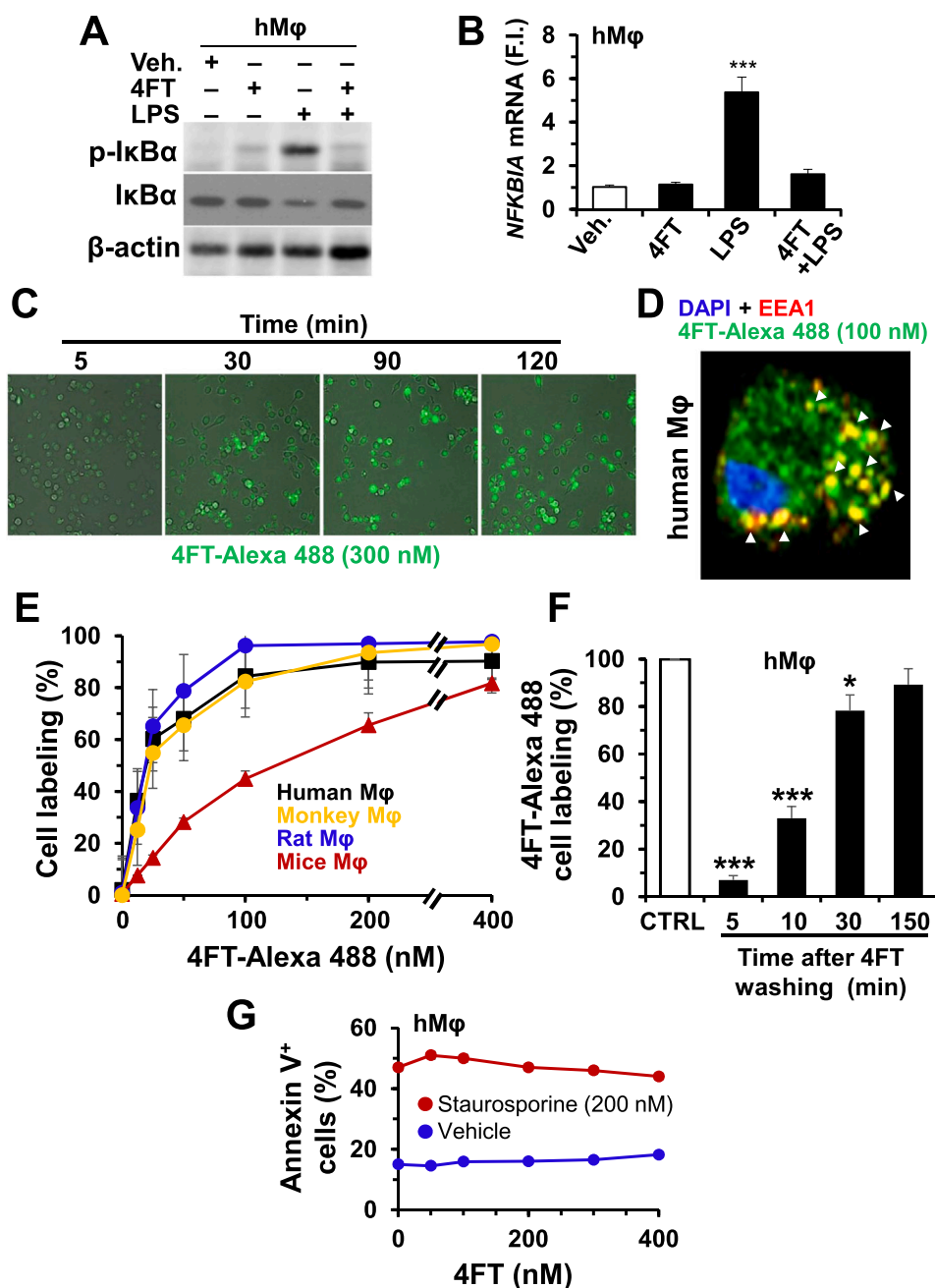
Fig. 1. Treatment of macrophages with 4FT inhibits LPS-dependent TLR4 signaling and promotes internalization of the 4FT-TLR4 complex. (A) Human macrophages (hMφ) were treated with 4FT (100 nM) and LPS (100 ng/ml) and the phosphorylation and total levels of IκBα were determined after 10 min of incubation. (B) The mRNA levels of *NFKBIA* were determined after 1 h of treatment of hMφ with 4FT (100 nM) and LPS (100 ng/ml). (C) Time-course of the internalization of 4FT labeled with Alexa 488 (300 nM) in hMφ, and (D) co-localization with the early endosome marker EEA1 (Rab5 effector early endosome antigen 1); *white arrowheads show colocalization of 4FT-Alexa 488 with EEA1.* (E) Dose-dependent incorporation of 4FT-Alexa 488 in primary cultures of macrophages from different species (10 min of incubation). (F) Re-exposure of TLR4 in the cell membrane of hMφ. Cells were treated with 100 nM 4FT for 10 min. After extensive washing of the cells to remove extracellular 4FT, cells were incubated for 10 min with 4FT-Alexa 488 at the indicated times after washing and the incorporation of the labeled 4FT was quantified by flow cytometry. Control (CTRL) refers to cells untreated with 4FT and challenged only with 4FT-Alexa 488. (G) Quantification of annexin V$^+$ cells treated for 18 h with the indicated concentrations of 4FT and the apoptosis-inducer staurosporine (200 nM). Results show representative blots and images (A, C, D) and the mean $\pm$ SD of five independent experiments. *P < 0.05, * **P < 0.005 *vs.* the corresponding 4FT vehicle (B) or cells untreated with 4FT (CTRL, panel F).

Parasternal short-axis-view images of the heart were recorded using a 30-MHz RMV scan head in B-mode to allow M-mode recordings by positioning the cursor in the parasternal short-axis view perpendicular to the interventricular septum and posterior wall of the left ventricle [33,34]. Left ventricle ejection fraction and fractional shortening were determined using the on-site software cardiac package (GE Healthcare).

2.6. Nitrite determination

NO synthesis by macrophages was evaluated spectrophotometrically from the amount of nitrites accumulated in the cell culture medium following a previous protocol [31].

2.7. Analysis of 4FT binding to TLR4 by flow cytometry

The indicated human, simian, mice, and rat cultured cells were

incubated with 4FT conjugated with 4FT-Alexa 488 and, after 10 min of incubation, were analyzed by flow cytometry (FACSCanto II; Beckton Dickinson; Madrid, ES) and positive cells were quantified using FlowJo software. DAPI (Life Technologies; Madrid, ES) was used to discriminate dead cells in the analysis. For cell counting, absolute counting beads were added (CountBright, Invitrogen).

2.8. Analysis of the subcellular distribution of 4FT

Time-lapse experiments were achieved by fluorescent microscopy (Cell Observer, Zeiss; Oberkochen, DE). Cells were incubated with 4FT-Alexa 488 and images were taken after 10 min of accommodation using a 25x objective (Plan-Apochromat 25x/0.8 oil immersion objective). Cells were fixed for 10 min at 20°C with 4% paraformaldehyde/0.1 M PBS (pH 7.4), followed by permeabilization with 0.5% saponin for 10 min and incubation with blocking solution (1% BSA, 0.3 M glycine in
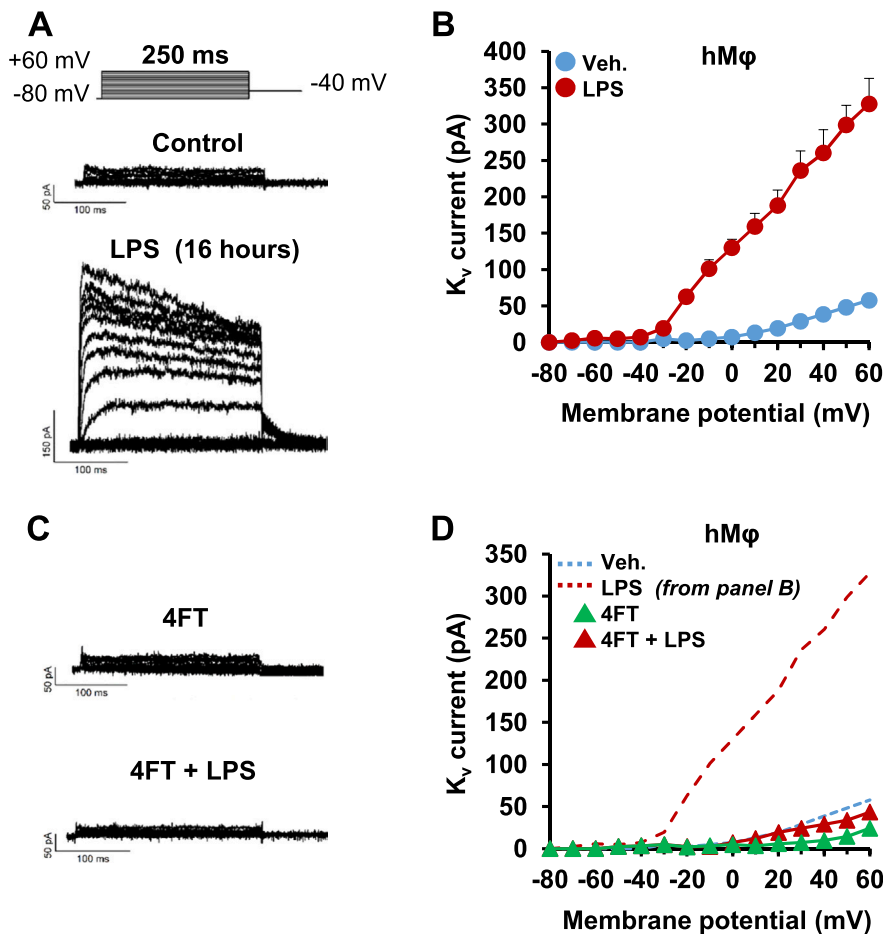
Fig. 2. 4FT inhibits the LPS-dependent rise in the Kv current of human macrophages. The Kv current generated by the Kv1.3/KV1.5 heterotetrameric channels was determined by patch-clamp analysis in cultured hMφ. (A-B) Cells were incubated for 16 h with 100 ng/ml of LPS and the Kv current was registered at different membrane potentials. (C-D) hMφ were treated for 1 h with 100 nM 4FT, followed by the addition of LPS (100 ng/ml). The Kv current was registered after 16 h of incubation with LPS (17 h with 4FT). Results show the mean $\pm$ SD of five independent experiments. *$P < 0.05$, *$P < 0.05$, *$P < 0.05$,.

PBS and 0.1% Tween). The primary antibody (Rab5 effector early endosome antigen 1, EEA1, in 1% BSA) was incubated in a humid chamber overnight at 4°C. Finally, cells were incubated with DAPI and prepared to be visualized, using Prolong (Invitrogen) as mounting medium, by confocal microscopy (LSM710-Zeiss).

2.9. TLR4 re-exposition kinetics and functional analysis of 4FT-TLR4 complexes

Cells were incubated with 100 nM 4FT for 10 min. After extensive cell washing to remove extracellular unbound 4FT, 100 nM 4FT-Alexa 488 was added at different times, and the incorporation of the labeled 4FT was followed by flow cytometry as previously described.

2.10. 4FT toxicity analysis

Different cell types were incubated for 18 h with increasing concentrations of 4FT and viability was determined by the incorporation of the tetrazolium dye MTT [3-(4,5-dimethylthiazol-2-yl)− 2,5-diphenyltetrazolium bromide] and by staining with annexin V as previously described [31]. Co-incubation of 4FT with staurosporine (200 ng/ml; Sigma) was used as a positive control of apoptosis-induction.

2.11. Determination of plasma membrane currents

Potassium currents were recorded at 20–25 °C and a frequency of 0.1 Hz using the whole-cell patch-clamp technique with an Axopatch 200B patch-clamp amplifier (Molecular Devices, San Jose, CA), following previous protocols [35]. The intracellular solution contained (in mM): 80 K-aspartate, 42 KCl, 3 phosphocreatine, 10 KH_2PO_4, 3 MgATP, 5 HEPES-K, 5 EGTA-K; pH 7.25 with KOH. Macrophages were superfused with an external solution containing (in mM): 136 NaCl, 4 KCl, 1.8 $CaCl_2$, 1 $MgCl_2$, 10 HEPES-Na and 10 glucose; pH 7.40 with NaOH. Cells were pre-incubated for 1 h with 100 nM 4FT, and then 20 ng/ml LPS was added to the external solution and incubated for 16 h. Origin 8.5 (OriginLab, Northampton, MA) and Clampfit 10 (Molecular Devices) programs were used to perform least-squares fitting and for data presentation.

2.12. Protein extraction and Western blot analysis

Cells or tissues were homogenized in a buffer containing 10 mM Tris-HCl, pH 7.5; 1 mM $MgCl_2$, 1 mM EGTA, 10% glycerol, 0.5% CHAPS and a protease and phosphatase inhibitor cocktail (Sigma). The extracts were vortexed for 30 min at 4°C and after centrifuging for 20 min at 13,000 *g*, the supernatants were stored at − 20°C. Protein levels were determined using Bradford reagent (Bio-Rad). Equal amounts of proteins (30 μg) were subjected to 10% SDS-PAGE electrophoresis gels. Proteins were transferred into polyvinylidene difluoride (PVDF) membranes (Bio-Rad). Membranes were incubated for 1 h with non-fat milk powder (5%) in PBS containing 0.1% Tween-20. Blots were incubated overnight at 4°C with primary antibodies at the dilutions recommended by the suppliers. Proteins were visualized using HRP-conjugated secondary antibodies. Blots were developed by ECL protocol and different exposition times were performed for each blot to ensure the linearity of the band intensities [31]. Values of densitometry were normalized for lane charge using antibodies against the corresponding loading control and densitometry was determined using Image J software.
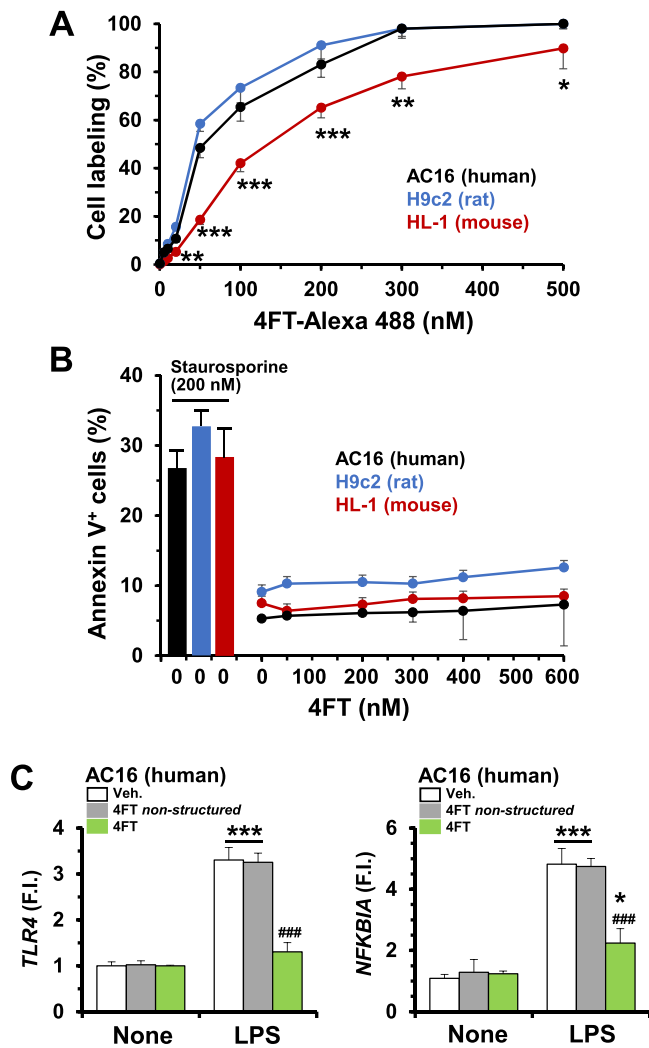
Fig. 3. Dose-dependent incorporation of 4FT in cardiomyocytic cell lines and effects on TLR4 activation. The human, rat, and mouse-derived cardiomyocytic cell lines AC16, H9c2 and HL-1, respectively, were incubated with different concentrations of 4FT or 4FT labeled with Alexa 488. (A) Flow cytometry analysis of the dose-dependent incorporation of 4FT-Alexa 488 after 10 min of incubation. (B) Effect of 4FT on the viability of the cardiomyocytic cell lines. Cells were incubated for 24 h with different concentrations of 4FT and the percentage of annexin V$^+$ cells was determined by flow cytometry. As a positive control, cells were treated for 24 h with staurosporine 200 nM to induce apoptosis. (C) The human cardiomyocytic cell line AC16 was treated for 8 h with 100 nM of 4FT or the same amount of non-structured aptamer as control, and 100 ng/ml of LPS. The mRNA levels of *TLR4* and *NFKBIA* were determined by real-time RT-PCR. Results show the mean $\pm$ SD of four (A,B) and six (C) independent experiments. *P < 0.05, **P < 0.01, ***P < 0.005 *vs.* AC16 cells (A) or *vs.* the corresponding condition in the absence of LPS (C). $^{\#\#\#}$P < 0.005 *vs.* the LPS condition in the absence of 4FT (C).

2.13. Histological analysis of cardiac lesion area

Rats were sacrificed and reperfused hearts were immediately fixed with formaldehyde, embedded in paraffin, cut into 3-μm-thick transverse sections, and stained with hematoxylin/eosin (H&E, Sigma) to evaluate the heart lesion. Picrosirius Red (Sigma) staining was performed to determine the collagen content in selected slides where the maximal I/R injury was observed. Images were quantified using ImageJ software.

2.14. Assay of myeloperoxidase (MPO) activity

MPO activity was measured in homogenized heart extracts (80 μg of protein in 200 μl of 10 mM Tris-HCl, pH 7.5; 1 mM MgCl$_2$, 1 mM EGTA, and a protease and phosphatase inhibitor cocktail from Sigma) centrifuged at 15,000 **g**. Aliquots of supernatants (50 μl) were assayed in a reaction mixture that contained 110 μl PBS, 20 μl of 0.22 M NaH$_2$PO$_4$ (pH 5.4), 20 μl of 0.026% (vol/vol) H$_2$O$_2$, and 20 μl of 18 mM tetramethylbenzidine in 8% (vol/vol) of aqueous dimethylformamide. After 15 min of reaction at 37 ºC, 30 μl of sodium acetate (1.5 M; pH 3) were added, and the absorbance at 620 nm was read in a microtiter plate reader. The activity was expressed as mU/g of tissue [36].

2.15. Analysis of immune cell infiltration by flow cytometry

Flow cytometry was used to evaluate differences between treatments in white cell counts in the heart. Rats were anesthetized with sodium pentobarbital (100 mg/kg i.p.) and heparinized (4 UI/g i.p.). Hearts were harvested and cannulated *via* the ascending aorta for Langerdorff perfusion in Tyrode solution containing 450 U/ml of collagenase I, 60 U/ml of hyaluronidase type I-S, and 60 U/ml of DNase-I, as previously described [37] The resulting cell suspension was dispersed by pipetting, filtered through a 250 mm nylon mesh and centrifuged for 4 min at 200 **g**. The cells were resuspended in HBSS (Thermo Fisher) supplemented with 10 mM HEPES and 0.5% fatty acid-free fraction V of bovine serum albumin (pH 7.4), incubated for 30 min at 4 °C with specific anti-rat antibodies and analyzed by flow cytometry following previous protocols [38,39]. Briefly, the CD45 population was labeled with APC-Cy7-conjugated anti-rat CD45 mAb (1:200; BioLegend, San Diego, CA, USA); the CD4 population with FITC-conjugated anti-rat CD4 mAb (1:100; BioLegend), and the CD11b/c cells with PE-conjugated anti-rat CD11b/c mAb (1:100; BioLegend). Flow cytometry was conducted in a FACSCanto II (Becton Dickinson), and the different cell subsets were defined using FlowJo software (Treestar, Ashland, OR, USA). For cell counting, absolute counting beads were added (CountBright, Invitrogen).

2.16. Myocardial apoptosis determination by fluorometric Terminal deoxynucleotidyl transfer-mediated dUTP Nick End-Labelling (TUNEL) assay

TUNEL-positive cells were quantified in isolated cardiac cells as described in the previous section and fixed cardiac sections as follows: The heart was harvested and rinsed with PBS. The organ was perfused through the aorta and cells were isolated in Langerdorff perfusion cut into 3 slides and immediately fixed with formaldehyde. The fixed tissue was embedded in paraffin and cut into 3-μm-thick transverse sections. TUNEL assays in isolated cells and heart slides were carried out using a fluorescein-based Cell Death Detection Kit (11684795910, Roche), following the instructions of the supplier. Hearts were also incubated with DAPI solution (1:500) for 10 min and Prolong (Invitrogen) was used as the mounting medium. Images were analyzed using ImageJ.

2.17. Biochemical analysis of serum

Troponin I level in serum was determined as a marker of myocardial injury, using the STAT High-Sensitive troponin I assay (Abbott Diagnosis; Madrid, ES). Plasmatic brain natriuretic peptide (BNP) levels were determined using the RayBio Immunoassay (Raybiotech; Peachtree Corners, GA, USA) following the manufacturer's instructions. Other tissue injury indicators were LDH and AST activities, using commercial kits (LDH: 11581; AST: 11830, BioSystems, Gerona, ES). The levels of lipoxin A4 (LXA4) and resolvin D1 (RvD1) were measured in serum using specific ELISA kits (Cayman; Barcelona, ES), and following the instructions of the supplier.
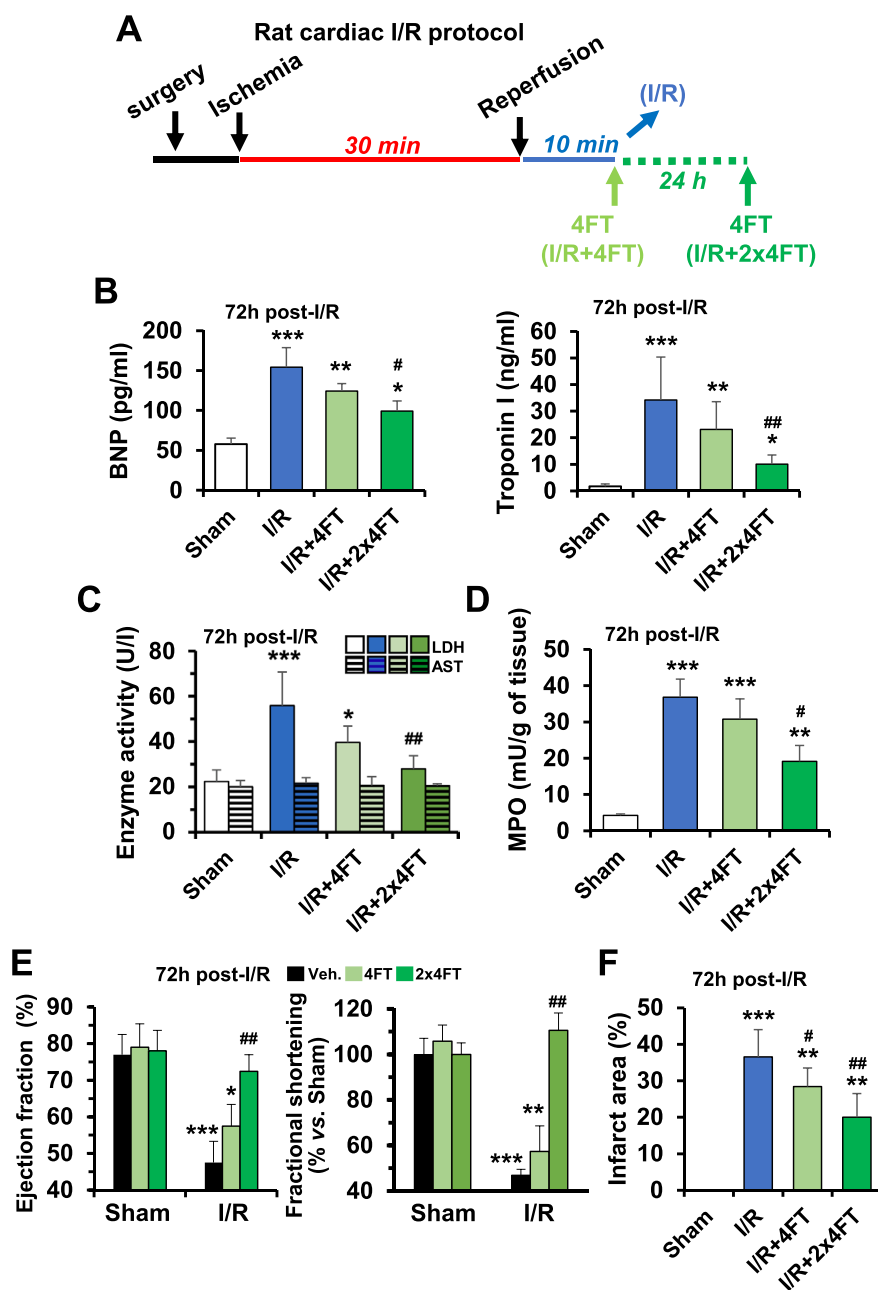
Fig. 4. Administration of 4FT to rats following cardiac ischemia/reperfusion (I/R) exerts significant protection against heart injury. (A) Rats were submitted to the described I/R protocol. Following reperfusion, rats received 20 nmol/kg body weight of 4FT *via* the tail vein 10 min after reperfusion (I/R+4FT group), or a second dose at 24 h post-reperfusion (I/R+2×4FT group). (B-D) Quantification of injury markers in serum of rats 72 h after reperfusion. (E-F) Effect of 4FT administration on the functional cardiac parameters and infarct size after I/R. Results show the mean $\pm$ SD of 12 animals for each condition. *P < 0.05, **P < 0.01, ***P < 0.005 *vs.* the Sham condition; #P < 0.05, ##P < 0.01 *vs.* the I/R condition (in the absence of 4FT administration).

2.18. Quantitative RT-PCR analysis

Total RNA was isolated from cells or hearts after perfusion through the left ventricle with PBS RNAse-free (ThermoFisher), by homogenization in QUIAZOL by a TissueLyser LT and eluted using MinElute columns (Qiagen, Madrid, ES). RNA integrity was assessed by RNA Nano Chip (Agilent; Madrid, ES). RNA was retro-transcribed by using the High-Capacity cDNA Reverse Transcription Kit (Applied Bioscience) and qRT-PCR was conducted using specific primers (ThermoFisher). Sequences are reported in Suppl. Table I. Calculations were made from the measurement of duplicates of each sample. The relative amount of mRNA was calculated with the comparative $2^{-\Delta\Delta Ct}$ method using rat *Rpl32* and human *RPLP0* as endogenous control transcripts.

2.19. Statistical analysis

Values in graphs correspond to the mean $\pm$ standard deviation (SD).

Statistical significance was estimated with two-tailed Student t-test for unpaired observations and one-way ANOVA for multiple comparisons followed by Tukey's range test as indicated under each figure. All analyses were performed using GraphPad Prism Software.

3. Results

3.1. Characterization of the binding of the aptamer 4FT to the TLR4 receptor

Since the aptamer 4FT was developed to bind the extracellular domain of the human TLR4 receptor, we first confirmed the antagonistic nature of 4FT over LPS-dependent TLR4 activation of human macrophages (hMφ) by following the phosphorylation of the TLR4 downstream kinase IKKα/β (a key regulator of the NF-κB pathway). As Suppl. Fig. S1 shows, incubation of hMφ with 4FT blunted the LPS-dependent phosphorylation of this kinase, which resulted in the absence of

phosphorylation and reduced proteolytic degradation of IκBα, one of its main substrates (Fig. 1 A). In agreement to this, incubation of hMφ with 4FT significantly prevented the LPS-dependent and the expression of NF-κB-dependent genes, such as *NFKBIA* (encoding IκBα; Fig. 1B).

Interestingly, after binding of 4FT to TLR4, the receptor is internalized (Fig. 1 C) and partially localized in early endosomes, as determined by the colocalization of 4FT with the Rab5 effector early endosome antigen 1 (EEA1, Fig. 1D). Furthermore, the labeling of different types of
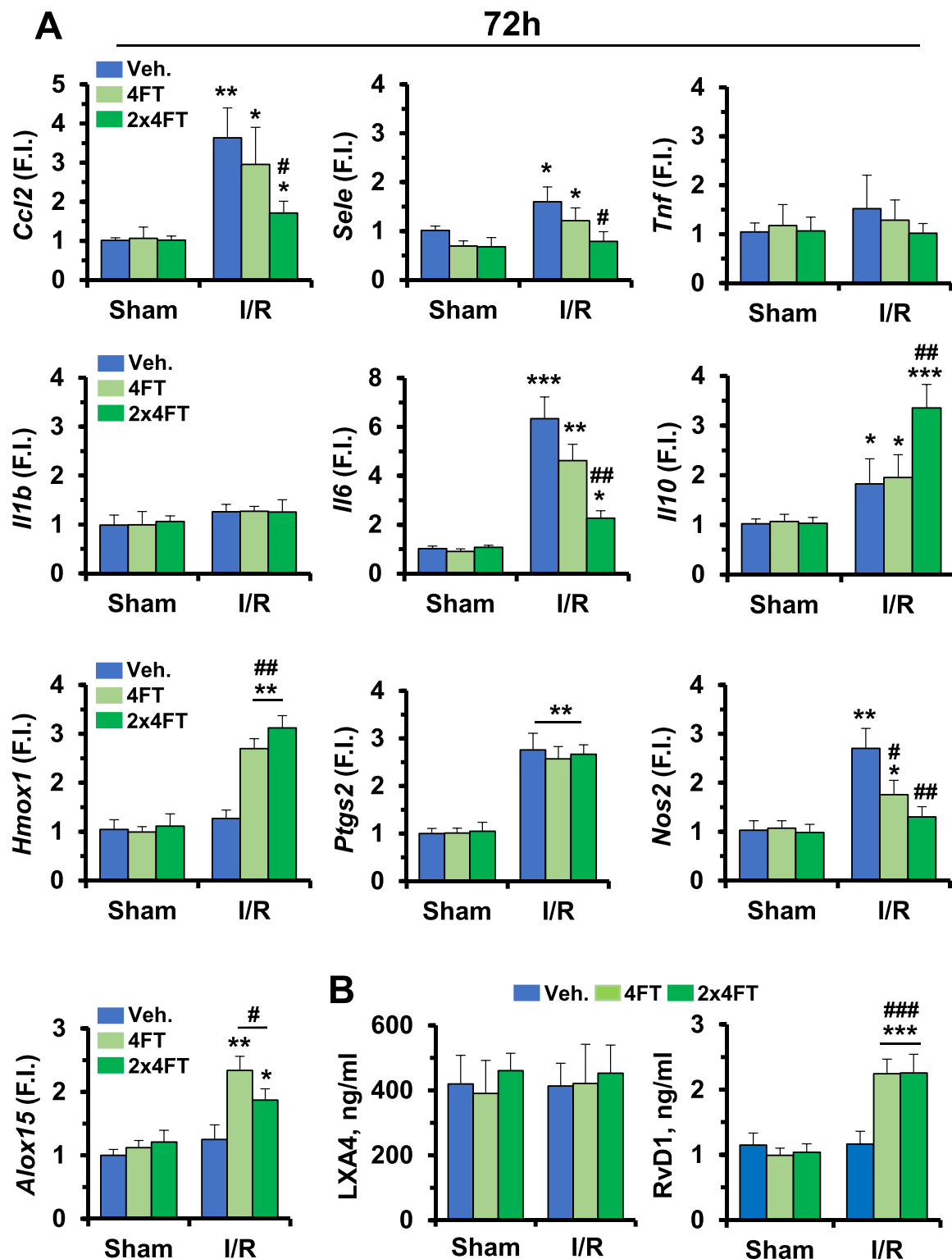

Fig. 5. Administration of 4FT to rats following cardiac ischemia/reperfusion (I/R) reduces the pro-inflammatory profile and favors the synthesis of pro-resolution lipid mediators. (A) Rats were submitted to the I/R protocol described in Fig. 4. The mRNA levels of the indicated genes were measured in the cardiac tissue by real-time quantitative RT-PCR. (B) The serum levels of the pro-resolution lipid mediators lipoxin A4 (LXA4) and resolvin D1 (RvD1) were quantified. Results show the mean $\pm$ SD of 8 animals for each condition (A), or 6 animals per condition assayed per triplicate (B). *P < 0.05, **P < 0.01, ***P < 0.005 *vs.* the Sham condition; #P < 0.05, ##P < 0.01, ###P < 0.005 *vs.* the I/R condition (in the absence of 4FT administration).

macrophages with 4FT (using 4FT-Alexa 488) shows apparent affinities from 30 to 40 nM (human, monkey and rats) to 140 nM in mice (Fig. 1E). The kinetics of the re-exposition of TLR4 in the cell membrane surface is shown in Fig. 1 F. 4FT does not promote macrophage cell death when assayed up to 400 nM. It does not modify the pro-apoptotic death induced by staurosporine either (Fig. 1 G). Moreover, treatment of murine or human macrophages with 4FT does not induce the synthesis of NO and significantly inhibited the LPS-induced NO production in murine cells (human macrophages did not express NOS2 after LPS challenge; Suppl. Fig. 2).

Since the plasma membrane Kv currents are modulated by TLR4 activation, we evaluated the effect of treatment with 4FT on these currents. Analysis of Kv currents in human macrophages reveals that incubation with 4FT minimally reduces the current but it significantly impairs the rise in the current induced by LPS (Fig. 2 A-D).

Analysis of the binding of 4FT to human, rat, and mouse cardiomyocytic cell lines shows a similar profile to macrophages from the same species (Fig. 3 A; apparent 50% labeling: 50, 45 and 137 nM, respectively). Also, 4FT does not alter the cell viability of these cardiomyocytic cell lines (Fig. 3B) but it impairs the expression of *TLR4* and *NFKBIA* in the human cardiomyocytic cell line AC16 after treatment with LPS (Fig. 3 C); in this case, non-structured 4FT aptamer, used as a control to ensure the specificity of the structured molecule, failed to inhibit the response to LPS in these cells (Fig. 3 C).

3.2. Administration of 4FT after rat cardiac ischemia/reperfusion reduces post-myocardial infarction injury

Having shown that the affinity of TLR4 for 4FT in rat cells is similar to the human counterparts, we chose the use of the acute myocardial infarction (MI) ischemia/reperfusion (I/R) model described in Fig. 4 A. In this model, 4FT was administered 10 min after reperfusion and, in other cases, a second dose was administered 24 h after reperfusion. As Fig. 4B, C show, single addition of 4FT reduced the levels of the injury markers BNP (Brain Natriuretic Peptide), troponin I and LDH. Other injury markers, such as AST, which is more related to liver injury, remained unchanged across the treatments (Fig. 4 C). This protective effect of 4FT was significantly accentuated when a second dose of 4FT was administered at 24 h post-reperfusion, including a reduction of myeloperoxidase activity in the heart (Fig. 4D), an increase in the cardiac ejection fraction and the value of the fractional shortening (Fig. 4E), and a reduction in the infarct size (Fig. 4 F).

At the transcriptomic level, the treatment of rats with 4FT after myocardial I/R has an impact at 24 h on the reduction of *Nppb* (encoding BNP), *Tlr4* and genes associated with the pro-inflammatory profile, such as *Tnf, Il1b, Il6, Nfkb1* and *Nfkbia*, or the mRNA encoding NOS2 or COX2 (Suppl. Fig. S3). However, the effect on the transcription of anti-inflammatory genes, such as *Il10* is not evident (Suppl. Fig. S3). Analysis at 72 h post-I/R allows the evaluation of the single *vs.* the two-doses administration of 4FT. Fig. 5A shows that the mRNA levels of *Ccl2, Il6* and *Nos2* evidence a reduction in the two-doses model, suggesting that infiltration and activation of immune cells are significantly attenuated after two-doses administration of 4FT. Interestingly, the mRNA levels of *Il10* (involved in the induction of an anti-inflammatory phenotype), and also those of *Hmox1* (encoding heme oxygenase 1), *Ptgs2* and *Alox15* (encoding lipoxygenase 15, an enzyme involved in the biosynthesis of lipid pro-resolution mediators; SPM) were enhanced. For this reason, the levels of the SPMs lipoxin A4 (LXA4), derived from arachidonic acid, and resolvin D1 (RvD1), derived from the *n-3* docosahexaenoic acid, were measured to evaluate their potential contribution to the resolution of the inflammation after MI. As Fig. 5B shows, no statistically significant differences in the serum levels of LXA4, but a significant increase of RvD1 after two doses of 4FT was observed between the different groups studied.

Also, *Nppb* mRNA levels still show a significant reduction at 72 h after 4FT two-dose administration *vs.* the single administration. At 7 days after MI, *Nppb* mRNA returned to basal (Suppl. Fig. S4). Other genes involved in collagen synthesis (*Col1a1* and *Col3a1*) exhibited a reduction *vs.* the MI condition. The levels of *S100a4* (encoding the calcium-binding protein A4, a protein involved in the organization of the cytoskeleton) and *Acta2* (encoding the α-actin) decreased after 4FT administration. In addition to this, the elevation of *Tlr4* levels post-MI was suppressed after 4FT administration (Suppl. Fig. S4).

3.3. Treatment of rats with 4FT after myocardial infarction reduces cardiac infiltration of immune cells, apoptosis and fibrosis

Infiltration of circulating immune cells into the heart after I/R is one of the main factors governing the fate of the heart [3,40]. Quantification of cardiac immune cells on day 7 after I/R showed a significant reduction after treatment with a single dose of 4FT, an effect that was intensified after two doses of 4FT (Fig. 6A). In particular, the reduction of CD4+ and CD11b/c+ cells after two doses of 4FT generated a profile similar to the control group (Fig. 6A). Interestingly, this reduction in infiltrating cells is consistent with the decrease in MPO activity measured in heart extracts after 72 h post-MI and treatment with two doses of 4FT (Fig. 4D).

Blocking TLR4 with two-dose of 4FT after I/R reduced the extent of TUNEL+ cells in the heart at 72 h (Fig. 6B). This effect was more evident in samples obtained on day 7 after I/R, and a significant reduction in apoptotic cells was evident in rats treated with a single dose of 4FT (Fig. 6C).

Analysis of the hematoxylin/eosin staining of hearts post-MI shows a significant decrease in the lesion after administration of 4FT (Fig. 6D). This decrease in the injury was more evident after two-dose of 4FT (Fig. 6D). In addition to this, analysis of the fibrotic area with picrosirius Red confirms the reduction in the collagen scar in animals treated with two-doses of 4FT (Fig. 6D).

4. Discussion

Most CVDs are due to ischemic heart injury [41,42]. Cardiomyocytes use the oxidative metabolism of free fatty acids, triglycerides, and carbohydrates as the main source of energy [43,44]. Therefore, the deprivation of oxygen and nutrients results in a sudden interruption of the oxidative phosphorylation pathway and a decrease in ATP levels [45,46]. This ATP reduction provokes hypercontraction and cell death [47], leading to the activation of a 'sterile' inflammatory response [48–50], which promotes the infiltration and activation of immune cells in the re-perfused heart. In this scenario, TLR4 activation by damage-associated molecular pattern mediators (DAMPs) promotes the transcription of genes dependent on NF-κB [2,10,51,52]. Indeed, studies inhibiting or stimulating pharmacologically TLR4 activity showed the pivotal role of this receptor in the pathophysiology of CVDs. Myocardial I/R injury in *Tlr4* deficient mice, which show a lower inflammatory response with a decrease in NF-κB-dependent gene transcription is an example of this. These animals show a lower cardiac inflammatory infiltration and infarct size when compared with the *wild type* [8,53,54]. On the contrary, injection of the DAMP S100-A1, a TLR4 agonist associated with cardiac injury, enlarges infarct size and worsens left ventricle function [55]. Thus, one of the most promising strategies to minimize cardiac dysfunction after MI and other CVDs is through the control of the inflammatory onset, and TLR4 is considered a therapeutic target with the greatest clinical projection [17,28,56,57]. In this sense, the specific TLR4-antagonist aptamer 4FT, ApTOLL, is proposed as a pharmacological tool to block the action of TLR4, with several advantages over immunotherapeutic approaches that regulate this receptor [28,56]. Importantly, the aptamer 4FT, ApTOLL, is currently being developed in clinical trials. In a First-in-Human study, the aptamer showed a great safety profile and appropriate pharmacokinetics to be administered in acute indications such as myocardial infarction [27,57]. Following these results, two clinical trials are currently being developed
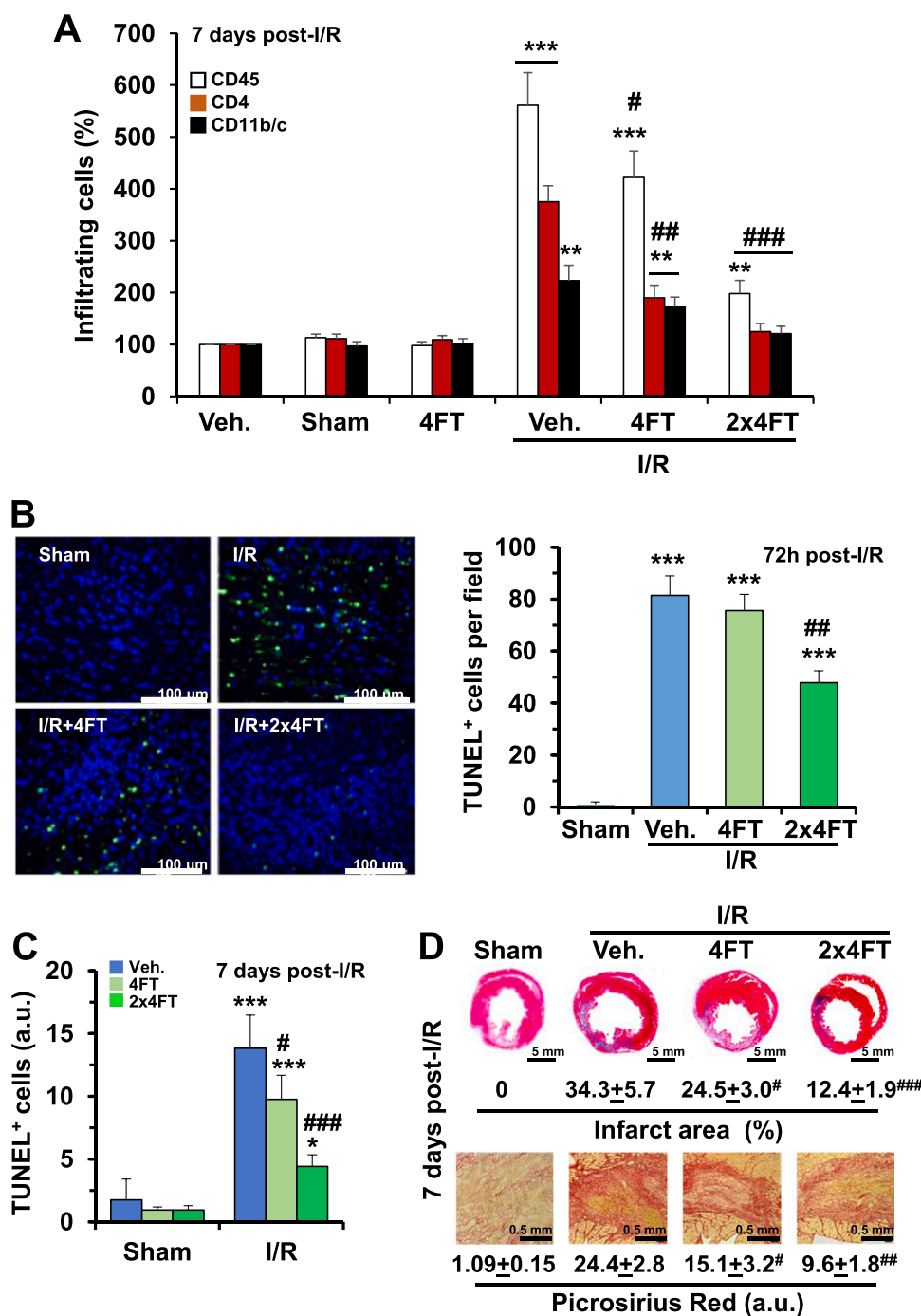
Fig. 6. 4FT administration to rats after cardiac ischemia/reperfusion (I/R) reduces the infiltration of circulating immune cells and protects against cardiac apoptosis and fibrosis. (A) Rats were submitted to the I/R protocol described in Fig. 4. The amount of CD45, CD4 and CD11b/c positive cells was determined by flow cytometry after digestion of the hearts, and data were referred to as percentage *vs.* the vehicle condition (in the absence of I/R). (B-C) Apoptosis was quantified by using the TUNEL assay kit in samples obtained at the indicated times. (D) Immunohistochemical analysis of cardiac injury after I/R. Hearts were stained with hematoxylin/eosin (upper panel), or with picrosirius Red to estimate the extent of fibrosis (lower panel). Results show the mean $\pm$ SD of 6 (Sham) and 7 animals for each I/R condition. *P < 0.05, * *P < 0.01, * **P < 0.005 *vs.* the Sham condition; #P < 0.05, ##P < 0.01, ###P < 0.005 *vs.* the I/R condition (in the absence of 4FT administration).

to assess safety and efficacy in acute stroke patients (APRIL trial: NCT04734548) and COVID-19 patients (APTACOVID trial; NCT05293236).

Characterization of the binding of the selective aptamer 4FT to TLR4 from hMφ showed a rapid internalization of the aptamer at the time that the LPS-dependent TLR4 signaling was significantly inhibited. This was confirmed by the reduced activity of the IKKα/β complex, resulting in the absence of IκBα phosphorylation and thus degradation by the ubiquitin/proteasome pathway, and the reduced expression of genes associated with TLR4 and TLR4-dependent NF-κB activation, such as *TLR4* and *NFKBIA*, and the blockade of the Kv current [58,59]. After this characterization, we analyzed the binding kinetics, functionality, and toxicity of the TLR4-specific 4FT aptamer in macrophages and cardiomyocytes from different species (human, simian, rat and mice). This

initial analysis confirmed the absence of 4FT toxicity in these cells and showed that the affinity of 4FT for the mice TLR4 was significantly lower than that of the rat and human counterparts (*ca.* one order of magnitude). For this reason, we decided to use the myocardial I/R model in rats, rather than mice.

After myocardial I/R, necrotic cardiomyocytes release DAMPs [60–62]. TLR4 activation by DAMPs is involved in the process of infiltration of immune cells through the upregulation of integrins and selectins by the endothelial and circulating cells, thus, activating the endothelial permeability and immune cell infiltration of the myocardium [63].

At this point, it is important to consider the kinetics of immune cell infiltration. This is because they can determine the protocol of 4FT administration. Given the re-exposition kinetics of TLR4 in hMφ treated

with 4FT (*ca.* 30 min), we considered comparing the effects of the single dose administered 10 min after reperfusion *vs.* a second dose administered 24 h later. As our data show, this two-dose administration of 4FT has a higher impact on the recovery after MI in almost all parameters evaluated. This is probably due to the modulation of the profile and intensity of the inflammatory cells recruited after cardiac injury. Indeed, the administration of a single dose of 4FT reduced *Tlr4* and *Nfkb1* levels in the infarcted hearts and showed a decrease in the mRNAs which encode chemoattractant molecules that promote the infiltration of inflammatory cells (*i.e.*, *Sele* and *Ccl2*) during the first 24 h; however, this protection in terms of apoptotic death was lesser than the two-dose protocol at 7 days.

The first immune cell type to infiltrate the injured area, especially at the ischemic border zone, are neutrophils, which reach a peak the day after reperfusion [64]. These neutrophils display an inflammatory activity, releasing reactive oxygen species and promoting MPO activity [65]. In fact, MPO cardiac activity is reduced after 4FT single-dose treatment, an effect enhanced in the two-dose protocol. Neutrophils contribute to the clearance of necrotic cells and tissue debris and the recruitment of monocytes into the infarcted area. These inflammatory monocytes in mice infiltrate during the first hours after the MI reaching a peak by days 3–4 [3,66,67]. Their efferocytotic activity and the release of anti-inflammatory cytokines such, as IL-10 and TGF-β favor the infiltration of inhibitory leukocyte subsets, reprogramming the transition and the secretion of anti-inflammatory mediators by survival cardiomyocytes of the survival zone [9,68]; hence, they stimulate the suppression of the pro-inflammatory response. From our results, 4FT administration, especially under the two-dose protocol, has a dual action: it promotes the release of anti-inflammatory mediators, such as IL-10, and at the same time favors the synthesis of pro-resolution lipid mediators, such as RvD1, contributing to the preservation of cardiac function, attenuation of the inflammatory response and adapting fibrosis to repair the damaged tissue [33,69,70]. Thus, a correct switch between the inflammatory and reparative response is necessary as it was described that depletion of neutrophils or macrophages induces greater damage [9,64,68]. Therefore, 4FT administration after I/R prevents an excessive infiltration and activation of leukocytes, which can induce cytotoxic injury by releasing ROS and proteolytic enzymes, not only in the infarcted area, but also in the viable tissue resulting in a secondary infarct extension, cardiac dysfunction and, finally, heart failure. Thus, the sum of the restricted capacity of the heart to regenerate and tolerate an extended inflammatory process makes it vulnerable to greater myocardial injury. In this regard, it is well known that short-term activation of innate immunity (preconditioning) confers adaptive and protective effects in the heart against subsequent and sustained ischemia [17,71]. However, long-term activation leads to maladaptive remodeling and worsens the situation leading to irreversible damage. Ischemic preconditioning (IPC) is based on brief episodes of repeated ischemia that protect the heart against a more severe and prolonged period of I/R.

5. Concluding remarks

According to our data, aptamer 4FT (ApTOLL), can be considered a candidate to attenuate TLR4 signaling with a significant security range. For this reason, clinical trials are in course to assess its use in inflammatory pathologies, such as stroke [28,56,57]. Therefore, 4FT can be added to a growing portfolio of TLR4 inhibitors and antagonists, including several clinical trials that have been done to target TLR4 activity (with low success up to now). This was the case of Eritoran, a synthetic lipidic TLR4 antagonist which was investigated as a possible treatment for sepsis but failed in phase III of the clinical trial [72]. However, apart from targeting sepsis, Eritoran could still be studied and used for therapy in other inflammatory diseases such as cardiac hypertrophy, where it demonstrated beneficial effects in an aortic constriction animal model [73]. In addition, other strategies targeting TLR4, such as the use of miR-135a, or NI-0101, a monoclonal anti-TLR4 antibody that

has been tested in clinical trials for the treatment of acute and chronic inflammation [74] opened new venues in protection against myocardial injury [75]. Indeed, in the field of MI, the possibility exists of combined myocardial revascularization by percutaneous coronary intervention, including thrombolytic therapy based on tissue plasminogen activator (tPA) administration and, as a novelty, targeting TLR4 activity as an emerging complementary approach.

In summary, this work provides experimental evidence for the use of the aptamer 4FT as a therapeutic alternative in the case of complex pathology such as MI. In addition, new studies are required to consider the administration of a second dose that maintains TLR4 inhibition for a longer period in these animal models to prevent the phase of tissue damage after I/R.

Statements and declarations

Ethics approval and consent to participate

Funding sources

Consent for publication

All authors concur and approve the submission of the manuscript.

Acknowledgments

Author contributions

M.P-G. and A.P-R. designed the study and performed experiments, analyzed data, designed the figures and revised the manuscript. R.I.J., C.Z., E.M.R-S. and D.A.P. designed and performed experiments, analyzed data and provided intellectual input and improvements. M.H-J., D.P. and I.L. provided intellectual input and improvements, discussed results and revised the manuscript. P.P., S.S-G., C.V., C.D provided intellectual input. M.L.G-B., M.A.M. and I.L. provided intellectual input and revised the manuscript. J.R. participated in immunohistochemistry experiments and provided intellectual input. L.B. wrote the paper, provided funding and intellectual input, discussed, and organized the information.

Conflict of interest

The authors have no relevant financial or non-financial interests to disclose. The information disclosed in this article is protected by the international patent application WO2015197706-A1 and its extensions to different countries; and by the international patent WO2020230109-A1.

Data Availability

Data will be made available on request.

Appendix A. Supporting information

Supplementary data associated with this article can be found in the online version at doi:10.1016/j.biopha.2023.114214.

References

[1] P. Zhou, W.T. Pu, Recounting cardiac cellular composition, Circ. Res. 118 (2016) 368–370, https://doi.org/10.1161/CIRCRESAHA.116.308139.

[2] N.G. Frangogiannis, The inflammatory response in myocardial injury, repair, and remodelling, Nat. Rev. Cardiol. 11 (2014) 255–265, https://doi.org/10.1038/nrcardio.2014.28.

[3] N. Haider, L. Boscá, H.R. Zandbergen, J.C. Kovacic, N. Narula, S. González-Ramos, M. Fernandez-Velasco, S. Agrawal, M. Paz-García, S. Gupta, K. DeLeon-Pennell, V. Fuster, B. Ibañez, J. Narula, Transition of macrophages to fibroblast-like cells in healing myocardial infarction, J. Am. Coll. Cardiol. 74 (2019) 3124–3135, https://doi.org/10.1016/j.jacc.2019.10.036.

[4] F.J. Carrillo-Salinas, N. Ngwenyama, M. Anastasiou, K. Kaur, P. Alcaide, Heart inflammation, Am. J. Pathol. 189 (2019) 1482–1494, https://doi.org/10.1016/j.ajpath.2019.04.009.

[5] P.C. Westman, M.J. Lipinski, D. Luger, R. Waksman, R.O. Bonow, E. Wu, S. E. Epstein, Inflammation as a driver of adverse left ventricular remodeling after acute myocardial infarction, J. Am. Coll. Cardiol. 67 (2016) 2050–2060, https://doi.org/10.1016/j.jacc.2016.01.073.

[6] G.P. van Hout, F. Arslan, G. Pasterkamp, I.E. Hoefer, Targeting danger-associated molecular patterns after myocardial infarction, Expert Opin. Ther. Targets 20 (2016) 223–239, https://doi.org/10.1517/14728222.2016.1088005.

[7] M.C. Basil, B.D. Levy, Specialized pro-resolving mediators: endogenous regulators of infection and inflammation, Nat. Rev. Immunol. 16 (2016) 51–67, https://doi.org/10.1038/nri.2015.4.

[8] M. Fernández-Velasco, S. González-Ramos, L. Boscá, M. Fernandez-Velasco, S. Gonzalez-Ramos, L. Bosca, Involvement of monocytes/macrophages as key factors in the development and progression of cardiovascular diseases, Biochem. J. 458 (2014) 187–193, https://doi.org/10.1042/BJ20131501.

[9] M. Horckmans, L. Ring, J. Duchene, D. Santovito, M.J. Schloss, M. Drechsler, C. Weber, O. Soehnlein, S. Steffens, Neutrophils orchestrate post-myocardial infarction healing by polarizing macrophages towards a reparative phenotype, Eur. Heart J. 38 (2016) 187–197, https://doi.org/10.1093/eurheartj/ehw002.

[10] Y. Yang, J. Lv, S. Jiang, Z. Ma, D. Wang, W. Hu, C. Deng, C. Fan, S. Di, Y. Sun, W. Yi, The emerging role of Toll-like receptor 4 in myocardial inflammation, Cell Death Dis. 7 (2016), e2234–e2234, https://doi.org/10.1038/cddis.2016.140.

[11] P.B. Katare, P.K. Bagul, A.K. Dinda, S.K. Banerjee, Toll-like receptor 4 inhibition improves oxidative stress and mitochondrial health in isoproterenol-induced cardiac hypertrophy in rats, Front. Immunol. 8 (2017) 719, https://doi.org/10.3389/fimmu.2017.00719.

[12] S. Goulopoulou, C.G. McCarthy, R.C. Webb, Toll-like receptors in the vascular system: sensing the dangers within, Pharmacol. Rev. 68 (2016) 142–167, https://doi.org/10.1124/pr.114.010090.

[13] N. Goren, J. Cuenca, P. Martin-Sanz, L. Bosca, Attenuation of NF-kB signalling in rat cardiomyocytes at birth restricts the induction of inflammatory genes, Cardiovasc. Res. 64 (2004) 289–297, https://doi.org/S0008-6363(04)00286-X [pii] 10.1016/j.cardiores.2004.06.029 [doi].

[14] J. Cuenca, N. Goren, P. Prieto, P. Martín-Sanz, L. Boscá, Selective impairment of nuclear factor-κb-dependent gene transcription in adult cardiomyocytes, Am. J. Pathol. 171 (2007) 820–828, https://doi.org/10.2353/ajpath.2007.061076.

[15] D.L. Mann, The emerging role of innate immunity in the heart and vascular system, Circ. Res. 108 (2011) 1133–1145, https://doi.org/10.1161/CIRCRESAHA.110.226936.

[16] J. Oyama, C. Blais, X. Liu, M. Pu, L. Kobzik, R.A. Kelly, T. Bourcier, Reduced myocardial ischemia-reperfusion injury in toll-like receptor 4-deficient mice, Circulation 109 (2004) 784–789, https://doi.org/10.1161/01.CIR.0000112575.66565.84.

[17] S.M. Lee, M. Hutchinson, D.A. Saint, The role of Toll-like receptor 4 (TLR4) in cardiac ischaemic-reperfusion injury, cardioprotection and preconditioning, Clin. Exp. Pharmacol. Physiol. 43 (2016) 864–871, https://doi.org/10.1111/1440-1681.12602.

[18] S. Frantz, L. Kobzik, Y.-D. Kim, R. Fukazawa, R. Medzhitov, R.T. Lee, R.A. Kelly, Toll4 (TLR4) expression in cardiac myocytes in normal and failing myocardium, J. Clin. Investig. 104 (1999) 271–280, https://doi.org/10.1172/JCI6709.

[19] J. Tian, X. Guo, X.-M. Liu, L. Liu, Q.-F. Weng, S.-J. Dong, A.A. Knowlton, W.-J. Yuan, L. Lin, Extracellular HSP60 induces inflammation through activating and up-regulating TLRs in cardiomyocytes, Cardiovasc. Res. 98 (2013) 391–401, https://doi.org/10.1093/cvr/cvt047.

[20] F. Lipi, S. Chen, M. Chakravarthy, S. Rakesh, R.N. Veedu, In vitro evolution of chemically-modified nucleic acid aptamers: pros and cons, and comprehensive selection strategies, RNA Biol. 13 (2016) 1232–1245, https://doi.org/10.1080/15476286.2016.1236173.

[21] S. Jain, J. Kaur, S. Prasad, I. Roy, Nucleic acid therapeutics: a focus on the development of aptamers, Expert Opin. Drug Discov. 16 (2021) 255–274, https://doi.org/10.1080/17460441.2021.1829587.

[22] J.G. Bruno, Applications in which aptamers are needed or wanted in diagnostics and therapeutics, Pharmaceuticals 15 (2022) 693, https://doi.org/10.3390/ph15060693.

[23] Z. Zhuo, Y. Yu, M. Wang, J. Li, Z. Zhang, J. Liu, X. Wu, A. Lu, G. Zhang, B. Zhang, Recent advances in SELEX technology and aptamer applications in biomedicine, Int. J. Mol. Sci. 18 (2017) 2142, https://doi.org/10.3390/ijms18102142.

[24] N. Bejar, T.T. Tat, D.L. Kiss, RNA therapeutics: the next generation of drugs for cardiovascular diseases, Curr. Atheroscler. Rep. 24 (2022) 307–321, https://doi.org/10.1007/s11883-022-01007-9.

[25] T.R. Damase, R. Sukhovershin, C. Boada, F. Taraballi, R.I. Pettigrew, J.P. Cooke, The limitless future of RNA therapeutics, Front. Bioeng. Biotechnol. 9 (2021), 628137, https://doi.org/10.3389/fbioe.2021.628137.

[26] D.H. Katz, J.M. Robbins, S. Deng, U.A. Tahir, A.G. Bick, A. Pampana, Z. Yu, D. Ngo, M.D. Benson, Z.-Z. Chen, D.E. Cruz, D. Shen, Y. Gao, C. Bouchard, M.A. Sarzynski, A. Correa, P. Natarajan, J.G. Wilson, R.E. Gerszten, Proteomic profiling platforms head to head: Leveraging genetics and clinical traits to compare aptamer- and antibody-based methods, Sci. Adv. 8 (2022) eabm5164, https://doi.org/10.1126/sciadv.abm5164.

[27] M. Liu, K. Zaman, Y.M. Fortenberry, Overview of the therapeutic potential of aptamers targeting coagulation factors, Int. J. Mol. Sci. 22 (2021) 3897, https://doi.org/10.3390/ijms22083897.

[28] G. Fernández, A. Moraga, M.I. Cuartero, A. García-Culebras, C. Peña-Martínez, J. M. Pradillo, M. Hernández-Jiménez, S. Sacristán, M.I. Ayuso, R. Gonzalo-Gobernado, D. Fernández-López, M.E. Martín, M.A. Moro, V.M. González, I. Lizasoain, TLR4-binding DNA aptamers show a protective effect against acute stroke in animal models, Mol. Ther. 26 (2018) 2047–2059, https://doi.org/10.1016/j.ymthe.2018.05.019.

[29] A. Povo-Retana, M. Mojena, A.B.A.B. Stremtan, V.B.V.B. Fernández-García, A. Gómez-Sáez, C. Nuevo-Tapioles, J.M.J.M. Molina-Guijarro, J. Avendaño-Ortiz, J.M.J.M. Cuezva, E. López-Collazo, J.F.J.F. Martínez-Leal, L. Boscá, Specific effects of trabectedin and lurbinectedin on human macrophage function and fate—novel insights, Cancers 12 (2020) 3060, https://doi.org/10.3390/cancers12103060.

[30] A. Povo-Retana, M. Mojena, A. Boscá, J. Pedrós, D.A. Peraza, C. Valenzuela, J. M. Laparra, F. Calle, L. Boscá, Graphene particles interfere with pro-inflammatory polarization of human macrophages: functional and electrophysiological evidence, Adv. Biol. 5 (2021) 2100882, https://doi.org/10.1002/adbi.202100882.

[31] J.C. Rodriguez-Prados, P.G. Traves, J. Cuenca, D. Rico, J. Aragones, P. Martin-Sanz, M. Cascante, L. Bosca, Substrate fate in activated macrophages: a comparison between innate, classic, and alternative activation, J. Immunol. 185 (2010) 605–614, https://doi.org/10.4049/jimmunol.0901698.

[32] I. Cuadrado, M. Fernández-Velasco, L. Boscá, B. de las Heras, Labdane diterpenes protect against anoxia/reperfusion injury in cardiomyocytes: involvement of AKT activation, Cell Death Dis. 2 (2011), e229–e229, https://doi.org/10.1038/cddis.2011.113.

[33] R.I. Jaén, M. Fernández-Velasco, V. Terrón, S. Sánchez-García, C. Zaragoza, N. Canales-Bueno, A. Val-Blasco, M.T. Vallejo-Cremades, L. Boscá, P. Prieto, BML-111 treatment prevents cardiac apoptosis and oxidative stress in a mouse model of autoimmune myocarditis, FASEB J. 34 (2020) 10531–10546, https://doi.org/10.1096/fj.202000611R.

[34] A. Val-Blasco, J.A. Navarro-García, M. Tamayo, M.J. Piedras, P. Prieto, C. Delgado, G. Ruiz-Hurtado, L. Rozas-Romero, M. Gil-Fernández, C. Zaragoza, L. Boscá, M. Fernández-Velasco, Deficiency of NOD1 improves the β-adrenergic modulation of Ca2+ handling in a mouse model of heart failure, Front. Physiol. 9 (2018), e702, https://doi.org/10.3389/fphys.2018.00702.

[35] C. Moreno, P. Prieto, Á. Macías, M. Pimentel-Santillana, A. de la Cruz, P.G. Través, L. Boscá, C. Valenzuela, Modulation of voltage-dependent and inward rectifier potassium channels by 15-Epi-Lipoxin-A 4 in activated murine macrophages: implications in innate immunity, J. Immunol. 191 (2013) 6136–6146, https://doi.org/10.4049/jimmunol.1300235.

[36] P.G. Traves, V. Pardo, M. Pimentel-Santillana, A. Gonzalez-Rodriguez, M. Mojena, D. Rico, Y. Montenegro, C. Cales, P. Martin-Sanz, A.M.M. Valverde, L. Bosca, P. G. Través, V. Pardo, M. Pimentel-Santillana, A. González-Rodríguez, M. Mojena, D. Rico, Y. Montenegro, C. Calés, P. Martín-Sanz, A.M.M. Valverde, L. Boscá, Pivotal role of protein tyrosine phosphatase 1B (PTP1B) in the macrophage response to pro-inflammatory and anti-inflammatory challenge, Cell Death Dis. 5 (2014), e1125, https://doi.org/10.1038/cddis.2014.90.

[37] I. Cuadrado-Berrocal, M.V. Gómez-Gaviro, Y. Benito, A. Barrio, J. Bermejo, M. E. Fernández-Santos, P.L. Sánchez, M. Desco, F. Fernández-Avilés, M. Fernández-Velasco, L. Boscá, B. De Las Heras, A labdane diterpene exerts ex vivo and in vivo cardioprotection against post-ischemic injury: Involvement of AKT-dependent mechanisms, Biochem. Pharmacol. 93 (2015) 428–439, https://doi.org/10.1016/j.bcp.2014.12.011.

[38] S. González-Ramos, V. Fernández-García, M. Recalde, C. Rodríguez, J. Martínez-González, V. Andrés, P. Martín-Sanz, L. Boscá, Deletion or inhibition of NOD1 favors plaque stability and attenuates atherothrombosis in advanced atherogenesis, Cells 9 (2020), e2067, https://doi.org/10.3390/cells9092067.

[39] S. Gonzalez-Ramos, M. Paz-Garcia, C. Rius, A. Del Monte-Monge, C. Rodriguez, V. Fernandez-Garcia, V. Andres, J. Martinez-Gonzalez, M.A. Lasuncion, P. Martin-Sanz, O. Soehnlein, L. Bosca, Endothelial NOD1 directs myeloid cell recruitment in atherosclerosis through VCAM-1, FASEB J. 33 (2019) 3912–3921, https://doi.org/10.1096/fj.201801231RR.

[40] J. Cuenca, P. Martín-Sanz, A.M. Álvarez-Barrientos, L. Boscá, N. Goren, Infiltration of inflammatory cells plays an important role in matrix metalloproteinase expression and activation in the heart during sepsis, Am. J. Pathol. 169 (2006) 1567–1576, https://doi.org/10.2353/ajpath.2006.060109.

[41] C. Varenhorst, P. Hasvold, S. Johansson, M. Janzon, P. Albertsson, M. Leosdottir, K. Hambraeus, S. James, T. Jernberg, B. Svennblad, B. Lagerqvist, Culprit and nonculprit recurrent ischemic events in patients with myocardial infarction: data from SWEDEHEART (Swedish Web System for Enhancement and Development of Evidence-Based Care in Heart Disease Evaluated According to Recommended Therapies), J. Am. Heart Assoc. 7 (2018), e7174, https://doi.org/10.1161/JAHA.117.007174.

[42] D.J. Hausenloy, D.M. Yellon, The therapeutic potential of ischemic conditioning: an update, Nat. Rev. Cardiol. 8 (2011) 619–629, https://doi.org/10.1038/nrcardio.2011.85.

[43] J. Mori, R. Basu, B.A. McLean, S.K. Das, L. Zhang, V.B. Patel, C.S. Wagg, Z. Kassiri, G.D. Lopaschuk, G.Y. Oudit, Agonist-induced hypertrophy and diastolic dysfunction are associated with selective reduction in glucose oxidation: a metabolic contribution to heart failure with normal ejection fraction, Circ. Heart Fail. 5 (2012) 493–503, https://doi.org/10.1161/CIRCHEARTFAILURE.112.966705.

[44] H. Taegtmeyer, M.E. Young, G.D. Lopaschuk, E.D. Abel, H. Brunengraber, V. Darley-Usmar, C. Des Rosiers, R. Gersztein, J.F. Glatz, J.L. Griffin, R.J. Gropler, H.-G. Holzhuetter, J.R. Kizer, E.D. Lewandowski, C.R. Malloy, S. Neubauer, L.R. Peterson, M.A. Portman, F.A. Recchia, J.E. Van Eyk, T.J. Wang, American Heart Association Council on basic cardiovascular sciences, assessing cardiac metabolism: a scientific statement from the American Heart Association, Circ. Res. 118 (2016) 1659–1701, https://doi.org/10.1161/RES.0000000000000097.

[45] W. Basu Ball, S. Kar, M. Mukherjee, A.G. Chande, R. Mukhopadhyaya, P.K. Das, Uncoupling protein 2 negatively regulates mitochondrial reactive oxygen species generation and induces phosphatase-mediated anti-inflammatory response in experimental visceral leishmaniasis, J. Immunol. 187 (2011) 1322–1332, https://doi.org/10.4049/jimmunol.1004237.

[46] D. Oleinikov, Myocardial Metabolism. In: Veterinary Anatomy and Physiology, in: IntechOpen, 2019: p. Ed: Rutland C. S., Kubale V. https://doi.org/10.5772/intechopen.80870.

[47] A.C. Cave, J.S. Ingwall, J. Friedrich, R. Liao, K.W. Saupe, C.S. Apstein, F.R. Eberli, ATP Synthesis During Low-Flow Ischemia, Circulation 101 (2000) 2090–2096, https://doi.org/10.1161/01.CIR.101.17.2090.

[48] N. Song, Z.-S. Liu, W. Xue, Z.-F. Bai, Q.-Y. Wang, J. Dai, X. Liu, Y.-J. Huang, H. Cai, X.-Y. Zhan, Q.-Y. Han, H. Wang, Y. Chen, H.-Y. Li, A.-L. Li, X.-M. Zhang, T. Zhou, T. Li, NLRP3 phosphorylation is an essential priming event for inflammasome activation, Mol. Cell. 68 (185–197) (2017), e6, https://doi.org/10.1016/j.molcel.2017.08.017.

[49] N. Kelley, D. Jeltema, Y. Duan, Y. He, The NLRP3 inflammasome: an overview of mechanisms of activation and regulation, Int. J. Mol. Sci. 20 (2019) 3328, https://doi.org/10.3390/ijms20133328.

[50] J. Zhou, Z. Zhou, X. Liu, H.-Y. Yin, Y. Tang, X. Cao, P2×7 receptor–mediated inflammation in cardiovascular disease, Front. Pharmacol. 12 (2021), e654425, https://doi.org/10.3389/fphar.2021.654425.

[51] D. De Kleijn, G. Pasterkamp, Toll-like receptors in cardiovascular diseases, Cardiovasc. Res. 60 (2003) 58–67, https://doi.org/10.1016/S0008-6363(03)00348-1.

[52] N.G. Frangogiannis, Regulation of the inflammatory response in cardiac repair, Circ. Res. 110 (2012) 159–173, https://doi.org/10.1161/CIRCRESAHA.111.243162.

[53] A. Riad, S. Jäger, M. Sobirey, F. Escher, A. Yaulema-Riss, D. Westermann, A. Karatas, M.M. Heimesaat, S. Bereswill, D. Dragun, M. Pauschinger, H.P. Schultheiss, C. Tschöpe, Toll-like receptor-4 modulates survival by induction of left ventricular remodeling after myocardial infarction in mice, J. Immunol. 180 (2008) 6954–6961, https://doi.org/10.4049/jimmunol.180.10.6954.

[54] S.M. Davidson, P. Ferdinandy, I. Andreadou, H.E. Bøtker, G. Heusch, B. Ibáñez, M. Ovize, R. Schulz, D.M. Yellon, D.J. Hausenloy, D. Garcia-Dorado, Multitarget strategies to reduce myocardial ischemia/reperfusion injury, J. Am. Coll. Cardiol. 73 (2019) 89–99, https://doi.org/10.1016/j.jacc.2018.09.086.

[55] D. Rohde, C. Schön, M. Boerries, I. Didrihsone, J. Ritterhoff, K.F. Kubatzky, M. Völkers, N. Herzog, M. Mähler, J.N. Tsoporis, T.G. Parker, B. Linke, E. Giannitsis, E. Gao, K. Peppel, H.A. Katus, P. Most, S100A1 is released from ischemic cardiomyocytes and signals myocardial damage via Toll-like receptor 4, EMBO Mol. Med. 6 (2014) 778–794, https://doi.org/10.15252/emmm.201303498.

[56] R. Ramirez-Carracedo, L. Tesoro, I. Hernandez, J. Diez-Mata, D. Piñeiro, M. Hernandez-Jimenez, J.L. Zamorano, C. Zaragoza, Targeting TLR4 with ApTOLL improves heart function in response to coronary ischemia reperfusion in pigs undergoing acute myocardial infarction, Biomolecules 10 (2020) 1167, https://doi.org/10.3390/biom10081167.

[57] M. Hernández-Jiménez, S. Martín-Vílchez, D. Ochoa, G. Mejía-Abril, M. Román, P. Camargo-Mamani, S. Luquero-Bueno, B. Jilma, M.A. Moro, G. Fernández,

[58] N. Villalonga, M. David, J. Bielanska, R. Vicente, N. Comes, C. Valenzuela, A. Felipe, Immunomodulation of voltage-dependent K+ channels in macrophages: molecular and biophysical consequences, J. Gen. Physiol. 135 (2010) 135–147, https://doi.org/10.1085/jgp.200910334.

[59] R. Vicente, A. Escalada, N. Villalonga, L. Texidó, M. Roura-Ferrer, M. Martín-Satué, C. López-Iglesias, C. Soler, C. Solsona, M.M. Tamkun, A. Felipe, Association of Kv1.5 and Kv1.3 contributes to the major voltage-dependent K+ channel in macrophages, J. Biol. Chem. 281 (2006) 37675–37685, https://doi.org/10.1074/jbc.M605617200.

[60] J.S. Roh, D.H. Sohn, Damage-associated molecular patterns in inflammatory diseases, Immune Netw. 18 (2018), e27, https://doi.org/10.4110/in.2018.18.e27.

[61] E.L. Goldberg, V.D. Dixit, Drivers of age-related inflammation and strategies for healthspan extension, Immunol. Rev. 265 (2015) 63–74, https://doi.org/10.1111/imr.12295.

[62] I. Fernández-Ruiz, F. Arnalich, C. Cubillos-Zapata, E. Hernández-Jiménez, R. Moreno-González, V. Toledano, M. Fernández-Velasco, M.T.T. Vallejo-Cremades, L. Esteban-Burgos, R. Pérez De Diego, M.A.A. Llamas-Matias, E. García-Arumi, R. Martí, L. Boscá, A.L.L. Andreu, J. López-Sendón, E. López-Collazo, I. Fernandez-Ruiz, F. Arnalich, C. Cubillos-Zapata, E. Hernandez-Jimenez, R. Moreno-González, V. Toledano, M. Fernandez-Velasco, M.T.T. Vallejo-Cremades, L. Esteban-Burgos, R.P. de Diego, M.A.A. Llamas-Matias, E. Garcia-Arumi, R. Marti, L. Bosca, A.L.L. Andreu, J.L. Lopez-Sendon, E. Lopez-Collazo, I. Fernandez-Ruiz, F. Arnalich, C. Cubillos-Zapata, E. Hernández-Jiménez, R. Moreno-González, V. Toledano, M. Fernandez-Velasco, M.T.T. Vallejo-Cremades, L. Esteban-Burgos, R. Pérez De Diego, M.A.A. Llamas-Matias, E. García-Arumi, R. Martí, L. Boscá, A.L.L. Andreu, J. López-Sendón, E. López-Collazo, Mitochondrial DAMPs induce endotoxin tolerance in human monocytes: an observation in patients with myocardial infarction, PLoS One 9 (2014), e95073, https://doi.org/10.1371/journal.pone.0095073.

[63] M.J.M. Silvis, S.E. Kaffka genaamd Dengler, C.A. Odille, M. Mishra, N.P. van der Kaaij, P.A. Doevendans, J.P.G. Sluijter, D.P.V. de Kleijn, S.C.A. de Jager, L. Bosch, G.P.J. van Hout, Damage-associated molecular patterns in myocardial infarction and heart transplantation: the road to translational success, Front. Immunol. 11 (2020), 599511, https://doi.org/10.3389/fimmu.2020.599511.

[64] S.-L. Puhl, S. Steffens, Neutrophils in post-myocardial infarction inflammation: damage vs. resolution? Front. Cardiovasc. Med. 6 (2019) 25, https://doi.org/10.3389/fcvm.2019.00025.

[65] Y. Döring, P. Libby, O. Soehnlein, Neutrophil extracellular traps participate in cardiovascular diseases, Circ. Res. 126 (2020) 1228–1241, https://doi.org/10.1161/CIRCRESAHA.120.315931.

[66] S.-H. Jung, B.-H. Hwang, S. Shin, E.-H. Park, S.-H. Park, C.W. Kim, E. Kim, E. Choo, I.J. Choi, F.K. Swirski, K. Chang, Y.-J. Chung, Spatiotemporal dynamics of macrophage heterogeneity and a potential function of Trem2hi macrophages in infarcted hearts, Nat. Commun. 13 (2022) 4580, https://doi.org/10.1038/s41467-022-32284-2.

[67] W.C. Poller, M. Nahrendorf, F.K. Swirski, Hematopoiesis and Cardiovascular Disease, Circ. Res. 126 (2020) 1061–1085, https://doi.org/10.1161/CIRCRESAHA.120.315895.

[68] Y. Ma, Role of neutrophils in cardiac injury and repair following myocardial infarction, Cells 10 (2021) 1676, https://doi.org/10.3390/cells10071676.

[69] R.I. Jaén, A. Val-Blasco, P. Prieto, M. Gil-Fernández, T. Smani, J.L. López-Sendón, C. Delgado, L. Boscá, M. Fernández-Velasco, Innate immune receptors, key actors in cardiovascular diseases, JACC Basic Transl. Sci. 5 (2020) 735–749, https://doi.org/10.1016/j.jacbts.2020.03.015.

[70] A. Val-Blasco, P. Prieto, R.I. Jaén, M. Gil-Fernández, M. Pajares, N. Domenech, V. Terrón, M. Tamayo, I. Jorge, J. Vázquez, A. Bueno-Sen, M.T. Vallejo-Cremades, J. Pombo-Otero, S. Sanchez-García, G. Ruiz-Hurtado, A.M. Gómez, C. Zaragoza, M.G. Crespo-Leiro, E. López-Collazo, A. Cuadrado, C. Delgado, L. Boscá, M. Fernández-Velasco, Specialized proresolving mediators protect against experimental autoimmune myocarditis by modulating Ca2+ handling and NRF2 activation, JACC Basic Transl. Sci. 7 (2022) 544–560, https://doi.org/10.1016/j.jacbts.2022.01.009.

[71] X. Rossello, A. Rodriguez-Sinovas, G. Vilahur, V. Crisóstomo, I. Jorge, C. Zaragoza, J.L.J.L. Zamorano, J. Bermejo, A. Ordoñez, L. Boscá, J. Vázquez, L. Badimón, F.M. F.M. Sánchez-Margallo, F. Fernández-Avilés, D. Garcia-Dorado, B. Ibanez, CIBER-CLAP (CIBERCV Cardioprotection Large Animal Platform): a multicenter preclinical network for testing reproducibility in cardiovascular interventions, Sci. Rep. 9 (2019) 20290, https://doi.org/10.1038/s41598-019-56613-6.

[72] F. Chen, L. Zou, B. Williams, W. Chao, Targeting toll-like receptors in sepsis: from bench to clinical trials, Antioxid. Redox Signal. 35 (2021) 1324–1339, https://doi.org/10.1089/ars.2021.0005.

[73] H. Ehrentraut, C. Weber, S. Ehrentraut, M. Schwederski, O. Boehm, P. Knuefermann, R. Meyer, G. Baumgarten, The toll-like receptor 4-antagonist

D. Piñeiro, M. Ribó, V.M. González, I. Lizasoain, F. Abad-Santos, First-in-human phase I clinical trial of a TLR4-binding DNA aptamer, ApTOLL: Safety and pharmacokinetics in healthy volunteers, Mol. Ther. Nucleic Acids 28 (2022) 124–135, https://doi.org/10.1016/j.omtn.2022.03.005.

eritoran reduces murine cardiac hypertrophy, Eur. J. Heart Fail. 13 (2011) 602–610, https://doi.org/10.1093/eurjhf/hfr035.

[74] E. Monnet, G. Lapeyre, E. van Poelgeest, P. Jacqmin, K. de Graaf, J. Reijers, M. Moerland, J. Burggraaf, C. de Min, Evidence of NI-0101 pharmacological activity, an anti-TLR4 antibody, in a randomized phase I dose escalation study in healthy volunteers receiving LPS, Clin. Pharmacol. Ther. 101 (2017) 200–208, https://doi.org/10.1002/cpt.522.

[75] H. Feng, B. Xie, Z. Zhang, J. Yan, M. Cheng, Y. Zhou, MiR-135a protects against myocardial injury by targeting TLR4, Chem. Pharm. Bull. 69 (2021) 529–536, https://doi.org/10.1248/cpb.c20-01003.